



## Simultaneous removal of sulfide, nitrate and acetate: Kinetic modeling

Aijie Wang<sup>a,\*</sup>, Chunshuang Liu<sup>a</sup>, Nanqi Ren<sup>a</sup>, Hongjun Han<sup>a</sup>, Duujong Lee<sup>a,b</sup>

<sup>a</sup> State Key Laboratory of Urban Water Resource and Environment, Harbin Institute of Technology (SKLUWRE, HIT), Harbin 150090, China

<sup>b</sup> Department of Chemical Engineering, National Taiwan University, Taipei 10617, Taiwan

### ARTICLE INFO

#### Article history:

Received 20 June 2009

Received in revised form

26 December 2009

Accepted 7 January 2010

Available online 15 January 2010

#### Keywords:

Denitrifying sulfide removal systems

Activated Sludge Model No. 1

Modeling

EGSB

### ABSTRACT

Biological removal of sulfide, nitrate and chemical oxygen demand (COD) simultaneously from industrial wastewaters to elementary sulfur ( $S^0$ ),  $N_2$ , and  $CO_2$ , or named the denitrifying sulfide (DSR) process, is a cost effective and environmentally friendly treatment process for high strength sulfide and nitrate laden organic wastewater. Kinetic model for the DSR process was established for the first time on the basis of Activated Sludge Model No. 1 (ASM1). The DSR experiments were conducted at influent sulfide concentrations of 200–800 mg/L, whose results calibrate the model parameters. The model correlates well with the DSR process dynamics. By introducing the switch function and the inhibition function, the competition between autotrophic and heterotrophic denitrifiers is quantitatively described and the degree of inhibition of sulfide on heterotrophic denitrifiers is realized. The model output indicates that the DSR reactor can work well at  $0.5 < C/S < 3.0$  with influent sulfide concentration of 400–1000 mg/L. At  $>1000$  mg/L influent sulfide, however, the DSR system will break down.

© 2010 Elsevier B.V. All rights reserved.

### 1. Introduction

Biological removal of sulfide, nitrate and chemical oxygen demand (COD) simultaneously from industrial wastewaters is a cost effective and environmentally friendly process. Autotrophic denitrifiers convert sulfide to  $S^0$  with available nitrate [1]. Wang et al. [2] developed a simultaneous de-sulfurization and denitrification (SDD) process utilizing a single autotrophic strain, *Thiobacillus denitrificans*, in a CSTR. Reyes-Avila et al. [3] achieved maximum removal rates for nitrogen, sulfide, and COD from a single CSTR of 0.209 kg-N/( $m^3$  d), 0.294 kg-S/( $m^3$  d), and 0.303 kg-C/( $m^3$  d), respectively. Chen et al. [4] utilized an expanded granular sludge bed (EGSB) reactor for simultaneous removal of sulfide, nitrate, and organic carbon at  $3.0$  kg-S  $m^{-3}$   $d^{-1}$ ,  $1.78$  kg-N/( $m^3$  d), and  $1.13$  kg-C/( $m^3$  d), respectively. A compromising balance between autotrophic and heterotrophic denitrifiers presents the prerequisite of success of the denitrifying sulfide removal (DSR) process. Competition between the autotrophic and heterotrophic denitrifiers under mixotrophic environment complicates system dynamics and appropriate control system design [3,5].

Biological models, such as Activated Sludge Model (ASM) or anaerobic digestion model (ADM) developed by International Water Association (IWA) [6–8], were developed to quantitatively describe the substrate degradation rates and the microbial growth rates in wastewater treatment processes [9,10]. However, the

models for DSR process are still lacking to the authors' best knowledge.

This paper aims at developing the biological model on the basis of ASM1 model for DSR tests conducted in an EGSB reactor operated at C/S ratio of 0.75–1.26 and at influent sulfide concentration of 200–800 mg/L. Then the calibrated model was utilized to quantitatively study the effects of C/S ratio and influent sulfide concentrations on DSR performance.

### 2. Materials and methods

#### 2.1. The EGSB reactor

The bench-scale EGSB reactor used in this study was refined from that used in Chen et al. [4] (Fig. 1). The EGSB reactor was made up of a plexiglass column with an internal diameter of 6 cm and a height of 180 cm. The working volume was 4.0 l (excluding head space). The bottom of the column, with a height of 5 cm, was the influent distributor. The middle part with a height of 140 cm and a height-per-diameter ratio of 23.33 was the DSR reaction zone filled with biological granules collected from an upflow anaerobic sludge blanket (UASB) reactor treating brewage wastewater of 70.6 mg/L suspended solids (SS) and 52.3 mg/L volatile suspended solids (VSS). The top, with a height of 35 cm, was the three-phase separator. An inverted funnel shaped gas separator was used to collect the produced biogas. A liquid upflow of 5 m/h was maintained for internal circulation. The EGSB reactor was kept at 30 °C. For the granules, the specific gravity was 1.065; the physical strength, expressed as integrity coefficient (the ratio of residual granules to

\* Corresponding author. Tel.: +86 451 86282195; fax: +86 451 86282195.

E-mail addresses: [waj0578@hit.edu.cn](mailto:waj0578@hit.edu.cn), [hitsrb@163.com](mailto:hitsrb@163.com) (A. Wang).

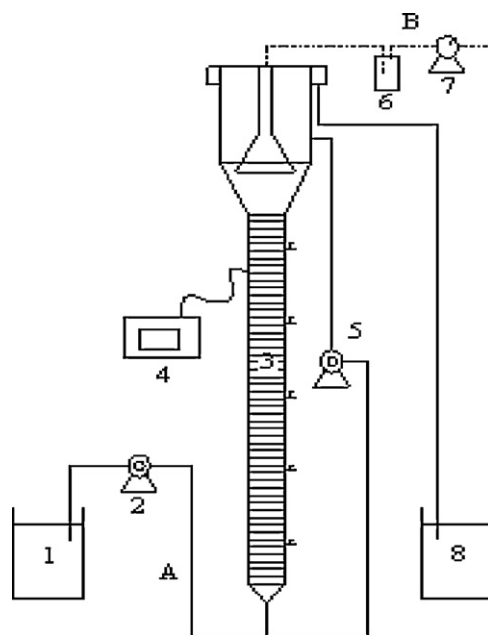


**Fig. 1.** The schematic of experimental reactor (1) feed tank, (2) influent pump, (3) EGSB reactor, (4) thermostat, (5) recycling pump, (6) gas sampler, (7) wet gas meter, (8) effluent water metering tank. A: water pipe, B: gas tube.

the total weight of the granular sludge after 5 min of shaking at 200 rpm on a platform shaker, expressed as percent), is higher than 95%. The reactor was set-up under mixotrophic conditions and during the whole process all sludge was stabilized. The influent sulfide and the ratio of C/S/N were 200 mg S/L and 1/1/1, respectively. The influent pH and hydraulic retention time maintained were 7.5 and (HRT) 10 h.

## 2.2. Tests

Experiments were conducted to study the effects of C/S and influent sulfide concentrations on the performance of the DSR-EGSB process. The effects of the ratios of C/S (0.75 mol/mol, 1.0 mol/mol and 1.26 mol/mol) were investigated with influent sulfide and nitrate concentrations of 400 mg S<sup>2-</sup>/L and 175 mg NO<sub>3</sub><sup>-</sup>-N/L (giving the S/N ratio of 1.0) at pH 7.5 controlled by hydrochloric acid and hydraulic retention time (HRT) 10 h. With prescribed C/S ratio, effects of sulfide concentrations on DSR process performance were studied at concentration of 200–800 mg/L for model calibration. During the study sodium sulfide, sodium nitrate and sodium acetate acted as sulfide, nitrate, and acetate, respectively. And the headspace above the medium was flushed with N<sub>2</sub> to exclude oxygen to prevent the chemical oxidation of sulfide supply.

## 2.3. Chemical analysis

An ion chromatography (Dionex ICS-3000, USA) measured the concentrations of acetate, nitrate, nitrite, sulfate, and thiosulfate in the collected liquor samples following 0.45- $\mu$ m filtration. Sample separation and elution were performed using an Ion-Pac AG4A AS4A-SC 4 mm analytical column (Dionex, USA) with carbonate/bicarbonate eluent (1.8 mmol/dm<sup>3</sup> Na<sub>2</sub>CO<sub>3</sub>/1.7 mmol/L NaHCO<sub>3</sub> at 1 cm<sup>3</sup>/min) and a sulfuric regeneration (H<sub>2</sub>SO<sub>4</sub>, 25 mmol/L at 5 cm<sup>3</sup>/min). The sulfide concentration was determined by potential titration using Sure-Flow™ Combination Silver/Sulfide Electrodes (Tianli Biochem, China). The solution alkalinity was measured via titration using diluted hydrochloric acid (HCl). A pH/ORP meter (pHS-25) determined the pH/ORP of the liq-

uid samples. The compositions in the gas phase were measured by a gas chromatography (Agilent 4980 DGC, USA). S<sup>0</sup> was qualitatively analyzed with hexahydropyridine and quantitative analyzed by sulfur balance analysis (defined as the percent of S<sup>0</sup> produced in the influent total sulfur).

## 3. Experimental results

### 3.1. Effects of C/S ratio

The reactor was under anaerobic conditions as indicated of  $-300$  mV ORP. Fig. 2 shows the sulfide, nitrate and acetate removal degree at C/S ratio 0.75–1.26 (stages I–III). At C/S=1.0, the sulfide, nitrate and acetate were completely removed. At C/S=0.75, the organic carbon was insufficient for nitrate removal via heterotrophic denitrification. Hence, a 90% (about 0.38 kg-N/(m<sup>3</sup> d)) nitrate-N removal rate was noted. At C/S=1.26, the heterotrophic denitrifiers overcompeted the autotrophic denitrifiers, yielding a 92% (about 0.89 kg-S/(m<sup>3</sup> d)) removal rate of sulfide-S. The last observation correlates with those by Oh et al. [11] and Lee et al. [12] that the presence of organic compounds enhances the nitrate removal under mixotrophic condition in a sulfur-utilizing autotrophic denitrification system.

In the present test N<sub>2</sub>O and nitrite accumulation were not noticeable, all nitrate reduced were converted to N<sub>2</sub>. There is no CH<sub>4</sub> produced, the organic substrate removal may mostly convert to CO<sub>2</sub>. And this result was conforming to the study of Chen et al. [4]. Additionally, the S<sup>0</sup> conversion rate was maintained at around 80% (0.77 kg-S/(m<sup>3</sup> d)). About 20% (0.19 kg-S/(m<sup>3</sup> d)) influent sulfides were converted to sulfate.

### 3.2. Effects of influent sulfide concentration

Fig. 3 shows the sulfide, nitrate and acetate removal degree with influent sulfide concentration of 200–800 mg/L. The C/S ratio was fixed at 1.0 and influent pH 7.5.

After the startup period, the EGSB reactor removed completely the sulfide-S, the acetate-COD, and the nitrate-N. Further increase in loading rates of sulfide, nitrate and acetate to 1.96 kg-S/(m<sup>3</sup> d), 0.84 kg-N/(m<sup>3</sup> d) and 0.72 kg-C/(m<sup>3</sup> d), did not reduce the removal rates. In most cases the sulfide was nearly completely converted to S<sup>0</sup> (Fig. 2a).

## 4. Kinetic model

### 4.1. Model development

The mathematical model for describing the reactor performance is implemented in the well-established AQUASIM simulation software [13]. The biological conversion processes were modeled using a modified ASM1 with a consideration of carbon removal and denitrification [7]. The established model is calibrated and used to simulate the biological reactions that occur in the DSR system, and the simulation results are compared with the experimental data obtained.

#### 4.1.1. Biological reactions

The present DSR model adopted modified ASM1 reaction scheme to account for the simultaneous COD oxidation and SDD processes using nitrifier, denitrifier and aerobic carbon removal bacteria. The denitrifiers, including autotrophic and heterotrophic counterparts, were active only under anaerobic condition. Autotrophic denitrifier conducted denitrification not ammonification reaction. The heterotrophic denitrifiers completed denitrification and carbon removal. A switch function was intro-

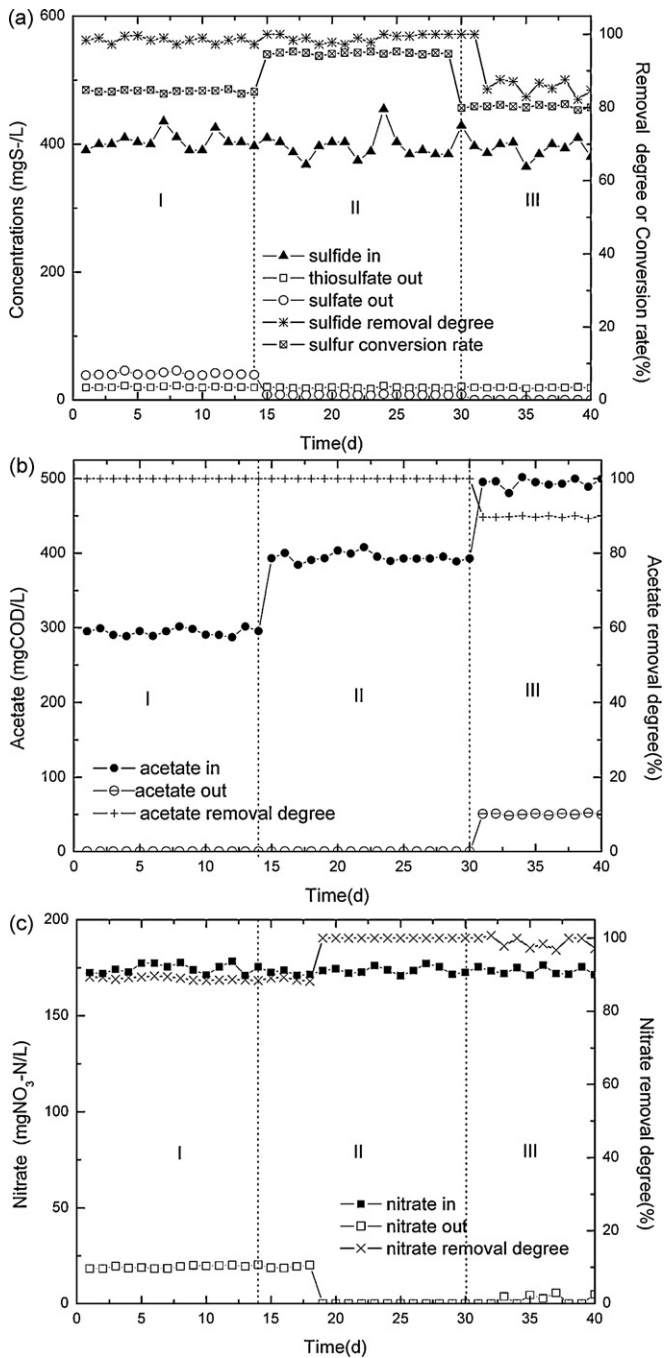


**Fig. 2.** Impact of C/S ratios on (a)  $S^{2-}$ , (b) acetate and (c)  $NO_3^-$ -N removal at C/S ratios of (I) 0.75/1, (II) 1/1, (III) 1.26/1.

duced to quantitatively describe the competition between the autotrophic and heterotrophic denitrifiers for nitrate (described later).

The DSR model has ten components, i.e., heterotrophic microorganisms ( $X_{B,H}$ ), autotrophic microorganisms ( $X_{B,A}$ ), readily biodegradable substrate ( $S_S$ ), soluble organic nitrogen ( $S_{ND}$ ), ammonia-N ( $S_{NH_3}$ ), nitrate-N and nitrite-N ( $S_{NO}$ ), particulate readily biodegradable organic nitrogen ( $X_{ND}$ ), slowly biodegradable organic substrate ( $X_S$ ), particulate substances produced by biomass attenuation ( $X_P$ ), sulfide-sulfur ( $S_{S^{2-}}$ ). This model has seven microbial processes: (1) growth of heterotrophic denitrifier, (2) growth of autotrophic denitrifier, (3) decay of heterotrophic denitrifier, (4) decay of autotrophic denitrifier, (5) ammonification of organic nitrogen, (6) hydrolysis of particulate organic carbon and (7)

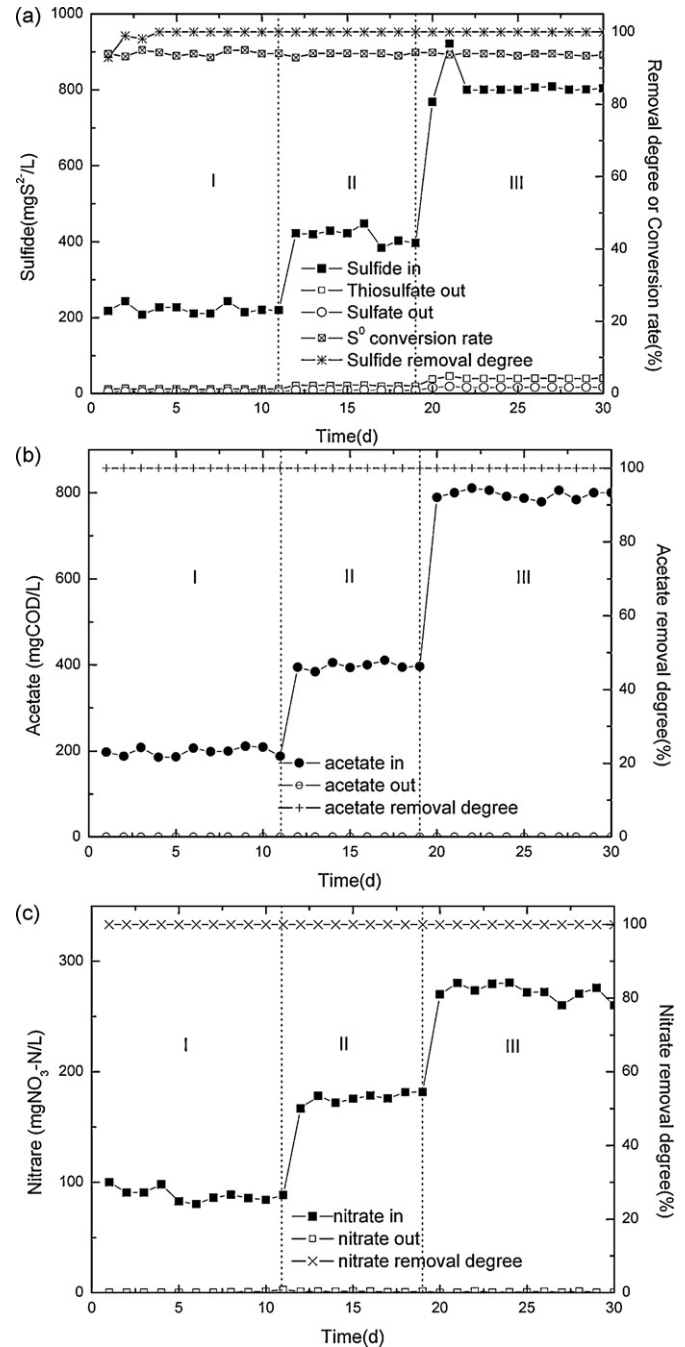


**Fig. 3.** Impact of influent sulfide on (a)  $S^{2-}$ , (b) acetate and (c)  $NO_3^-$ -N removal at  $S^{2-}$  concentrations of (I) 200 mg/L, (II) 400 mg/L and (III) 800 mg/L, respectively.

hydrolysis of particulate nitrogen. The structure of the proposed model is presented in Table 1. The tabular form indicates the changing rate (generation or utilization) of a model component for a given biochemical process can be obtained through multiplication of related process stoichiometry and kinetics [14,15].

#### 4.1.2. Switch function and inhibition function

The kinetic equations for autotrophic and heterotrophic denitrification are stated as follows [16]:

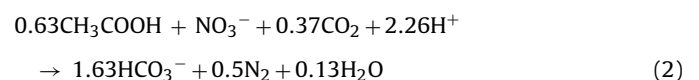
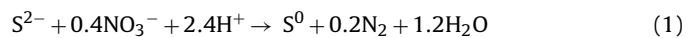


**Table 1**  
Stoichiometry and reaction kinetics of DSR system model.

| Process <i>j</i>   | Component <i>i</i>  |           |           |           |       |              |          |          |          |          | Reaction kinetics $\rho_j$<br>(mol <sup>-1</sup> s <sup>-1</sup> ) |
|--|---|-----------|-----------|-----------|-------|--------------|----------|----------|----------|----------|--|
|  | 1   | 2         | 3         | 4         | 5     | 6            | 7        | 8        | 9        | 10       |  |
|  | $S_S$   | $X_S$     | $X_{B,H}$ | $X_{B,A}$ | $X_P$ | $S_{S^{2-}}$ | $S_{NO}$ | $S_{NH}$ | $S_{ND}$ | $X_{ND}$ |  |
| 1  | -1/ $Y_H$   |           | 1         |           |       |              |          |          |          |          | $\rho_1$   |
| 2  |   |           |           | 1         |       | -2/ $Y_H$    |          |          |          |          | $\rho_2$   |
| 3  |   | $1 - f_p$ | -1        |           | $f_p$ |              |          |          |          |          | $\rho_3$   |
| 4  |   | $1 - f_p$ |           | -1        | $f_p$ |              |          |          |          |          | $\rho_4$   |
| 5  |   |           |           |           |       |              |          | 1        | -1       |          | $\rho_5$   |
| 6  | 1   | -1        |           |           |       |              |          |          |          |          | $\rho_6$   |
| 7  |   |           |           |           |       |              |          |          | 1        | -1       | $\rho_7$   |
| Reaction kinetics $\rho_j$<br>(mol <sup>-1</sup> s <sup>-1</sup> ) | $\rho_1 = \hat{\mu}_H \left( \frac{S_S}{K_S + S_S} \right) \left( \frac{N_S}{N_{S^{2-}} + N_S} \right) \left( \frac{S_{NO}}{K_{NO} + S_{NO}} \right) \eta_g X_{B,H}$ $\rho_2 = \hat{\mu}_A \left( \frac{S_{S^{2-}}}{S_{S^{2-}} + K_{S^{2-}}} \right) \left( \frac{N_{S^{2-}}}{N_S + N_{S^{2-}}} \right) \left( \frac{S_{NO}}{K_{NO} + S_{NO}} \right) X_{B,A}$ $\rho_3 = b_H X_{B,H}$ $\rho_4 = b_A X_{B,A}$ $\rho_5 = k_a S_{ND} X_{B,H}$ $\rho_6 = k_h \left( \frac{X_S / X_{B,H}}{K_X + (X_S / X_{B,H})} \right) \eta_h \left( \frac{S_{NO}}{K_{NO} + S_{NO}} \right) X_{B,H}$ $\rho_7 = \rho_6 \left( \frac{X_{ND}}{X_S} \right)$ |           |           |           |       |              |          |          |          |          |  |

We define the switch function as follows:

$$s' = \frac{N_S}{N_S + N_{S^{2-}}} \quad (3)$$

where  $N_S$  is the moles of nitrate consumed by sulfide according to Eq. (1), and  $N_{S^{2-}}$  is the moles of nitrate consumed by acetate according to Eq. (2). When autotrophic denitrifier significantly overcomes the heterotrophic denitrifier,  $s' \rightarrow 1$ ; conversely,  $s' \rightarrow 0$ . The switching function (Eq. (3)) describes the competition between the autotrophic and heterotrophic denitrifiers.

Another parameter, inhibition function ( $\eta_g$ ) was introduced to describe the inhibition of high strength sulfide (up to 800 mg/L) on heterotrophic denitrifier according to Chen et al. [4]. The inhibition function for ammonium and hydrogen on biological growth is refined as follows, to incorporate the observation by Chen et al. [4] that strain inhibition occurs at  $S^{2-} > 800$  mg/L:

$$\eta_g = \frac{1}{1 + (S_i - 0.8)/K_i} \quad @ S_i > 800 \text{ mg/L} \quad (4)$$

where  $S_i$  is the sulfide concentrations (g/L) of the DSR system, and  $K_i$  was the inhibition coefficient (g/L).

#### 4.1.3. The DSR model

The adopted EGSB reactor was operated under high recycling rate (recycle ratio 30:1), so the reactor was modeled as a completely mixed tank reactor (CSTR). Additionally, since the EGSB granules were not compact in interior structure, the biological reaction rates rather than substrate diffusional rates are taken as rate limiting steps for the studied system. Hence, the DSR-EGSB model is stated as follows:

$$V \frac{dS_i}{dt} = qS_{i,in} - qS_i + \sum_{j=1-10} \rho_j v_{i,j} \quad (5)$$

$$V \frac{dX_i}{dt} = qX_{i,in} - qX_i + \sum_{j=1-10} \rho_j v_{i,j} \quad (6)$$

**Table 2**  
Kinetic and process parameters used in simulations.

| Item                   | Parameters    | Definition  | Value | Unit   | References             |
|------------------------|---------------|---|-------|--|------------------------|
| Chemical stoichiometry | $Y_H$         | Heterotrophic yield coefficient from substrate  | 0.67  | gCOD g <sup>-1</sup> COD                           | [6,7,14]               |
|                        | $Y_A$         | Autotrophic yield coefficient   | 1.28  | gCOD g <sup>-1</sup> S                             | This work (calculated) |
|                        | $f_p$         | Inert fraction of biomass leading to particulate products                             | 0.08  | -  | [6,7,14]               |
|                        | $i_{XB}$      | Mass N/mass COD in biomass  | 0.084 | gN g <sup>-1</sup> COD                             | [6,7,14]               |
|                        | $i_{XP}$      | Mass N/mass COD in products from biomass  | 0.06  | gN g <sup>-1</sup> COD                             | [6,7,14]               |
| Kinetic parameters     | $\hat{\mu}_H$ | Maximum specific growth rate of substrate for heterotrophs                            | 4.0   | d <sup>-1</sup>                                    | [6,7,14]               |
|                        | $\hat{\mu}_A$ | Maximum specific growth rate of substrate for autotrophs                              | 4.25  | d <sup>-1</sup>                                    | This work (estimated)  |
|                        | $K_S$         | Substrate half-saturation coefficient for heterotrophic biomass                       | 3.8   | gCOD g <sup>-1</sup> m <sup>-3</sup>               | This work (estimated)  |
|                        | $K_{NO}$      | Nitrate half-saturation coefficient for heterotrophic biomass                         | 0.5   | NO <sub>3</sub> -N m <sup>-3</sup>                 | [6,7,14]               |
|                        | $b_H$         | Heterotrophic decay coefficient for formation of particulate                          | 0.3   | d <sup>-1</sup>                                    | [6,7,14]               |
|                        | $\eta_g$      | Correction factor for the growth of heterotrophs under high concentrations of sulfide | 1.0   | -  | [6,7,14]               |
|                        | $\eta_h$      | Correction factor for anoxic hydrolysis   | 0.8   | -  | This work(estimated)   |
|                        | $k_h$         | Maximum specific hydrolysis rate  | 3.0   | gCOD g <sup>-1</sup> COD d <sup>-1</sup>           | [6,7,14]               |
|                        | $K_X$         | Half-saturation coefficient for hydrolysis of particulate biodegradable substrate     | 0.1   | gCOD g <sup>-1</sup> COD                           | [6,7,14]               |
|                        | $k_a$         | Ammonification coefficient  | 0.05  | m <sup>3</sup> g <sup>-1</sup> COD d <sup>-1</sup> | [6,7,14]               |
|                        | $K'_{NO}$     | Nitrate half-saturation coefficient for autotrophic denitrifier                       | 0.01  | NO <sub>3</sub> -N m <sup>-3</sup>                 | This work (estimated)  |
|                        | $b_A$         | Autotrophic decay coefficient for formation of particulate                            | 0.05  | d <sup>-1</sup>                                    | [6,7,14]               |
|                        | $K_{S^{2-}}$  | Substrate half-saturation coefficient for autotrophic biomass                         | 14.64 | gS g <sup>-1</sup> m <sup>-3</sup>                 | This work (estimated)  |

The term  $\sum_{j=1-10} \rho_j v_{i,j}$  is the sum of the specific kinetic rates for process  $j$  multiplied by the associated stoichiometric coefficients (Table 2).  $V$  is the reactor volume,  $q$  is the influent and effluent of the reactor,  $S_{i,in}$  is the influent concentration of the soluble ( $X_{i,in}$  for the particulate) components and  $S_t$  is the soluble ( $X_i$  for the particulate) components in the reactor.

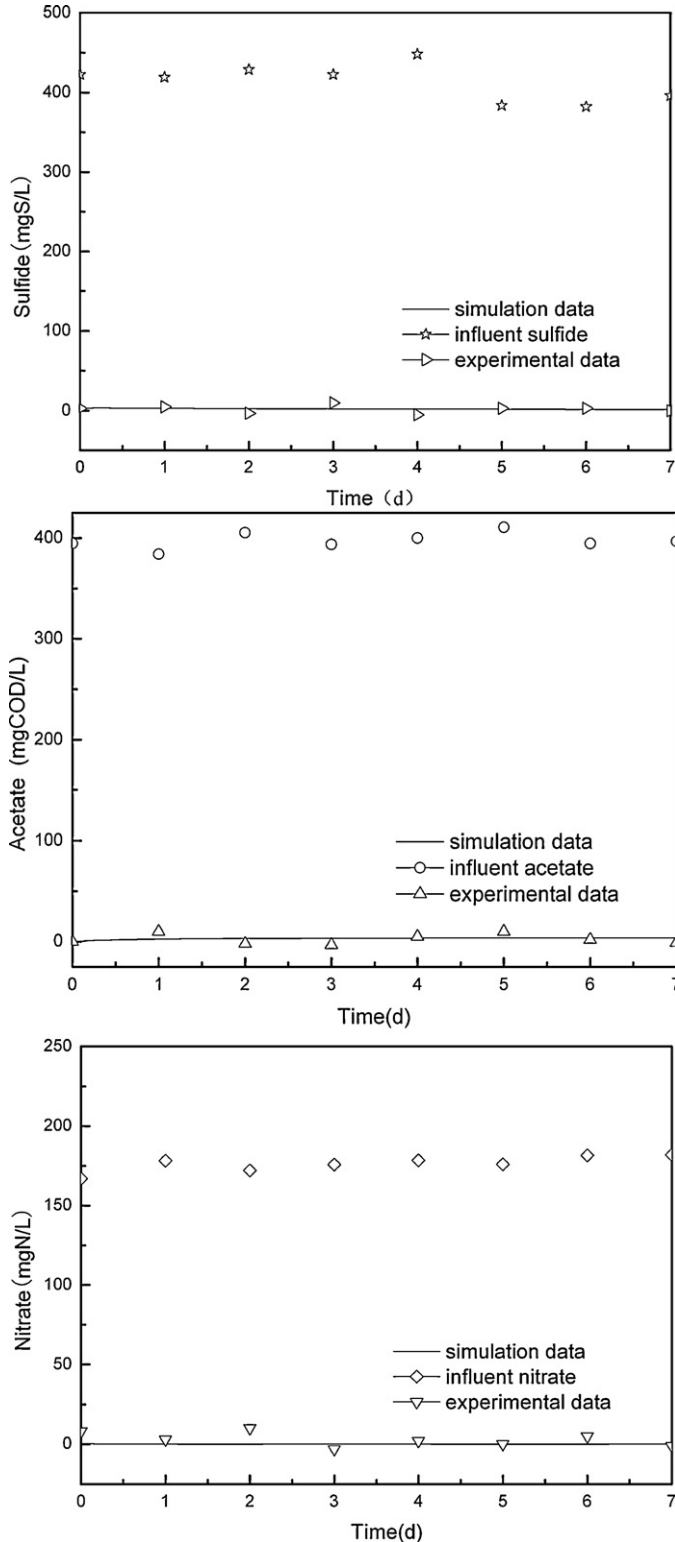


Fig. 4. Model validation results of the measured and simulated data for (a)  $S^{2-}$ , (b) acetate and (c)  $NO_3^-$ -N removal at  $S^{2-} = 400$  mg/L,  $C/S = 1$  and  $N/S = 1/1$ .

#### 4.2. Model calibration

The AQUASIM [13] is used to perform the model calibration for the established model. The parameter values are estimated by minimizing the sum of squares of the deviations between the measured data and predicted values.

The objective function to be minimized in the parameter estimation is as follows [17]:

$$F(p) = \left( \sum_{i=1}^n (y_{\text{exp},i} - y(p)_i)^2 \right)^{1/2} \quad (7)$$

where  $y_{\text{exp}}$  and  $y(p)$  are vectors of  $n$  measured value and model prediction at time  $t_i$  ( $i$  from 1 to  $n$ ), respectively, and  $p$  is the vector of the model parameters. In this study, the model is calibrated for the DSR system at influent sulfide of 200 mg  $S^{2-}$ /L and the ratio of  $C/N/S = 1/1/1$ . Preliminary numerical results for the established model revealed that the following five parameters,  $Y_a$ ,  $U_a$ ,  $K_s$ ,  $K_{S^{2-}}$  and  $K'_{NO_3}$ , mostly affected the COD,  $S^{2-}$ , and  $NO_3^-$ -N profiles measured. Hence, these five parameters were selected in model calibration. The steepest decent method was applied for parametric fitting. The estimated parameter values are summarized in Table 2.

Model verification is based on the comparison between the experimental results and model predictions under different input model parameters (400 mg  $S^{2-}$ /L, 87.5 mg  $NO_3^-$ -N/L and 75 mg Ac-C/L). The model satisfactorily describes the reactor dynamics (Fig. 4).

#### 5. Discussions

Influent sulfide concentration is an essential parameter for the DSR system for its inhibition role on heterotrophic. Moreover, both autotrophic denitrifier and heterotrophic denitrifier utilized nitrate as electron acceptors, then the competition of electron acceptors occurred while nitrate was limited. Autotrophic denitrifier utilized sulfide as electron donor, heterotrophic denitrifier utilized acetate as electron donor in the denitrifying sulfide removal system. So, the ratio of  $C/S$  influences the DSR performance. The model was used to predict DSR system performance at sulfide concentrations of 800–1100 mg/L (the ratio of the ratio of  $C/N/S = 1/1/1$ ) and  $C/S$  ( $C =$  carbon from acetate and  $S =$  sulfide and both in moles) of 0.5/1 to 3/1.

The sulfide concentration has adverse effects on the removal rates of sulfide, nitrate and acetate at  $S^{2-} > 1000$  mg/L (Fig. 5). At  $S^{2-} = 800$  mg/L, the acetate-COD, nitrate-N and sulfide were completely removed (about 1.92 kg- $S/(m^3$  d), 1.92 kg-COD/( $m^3$  d),

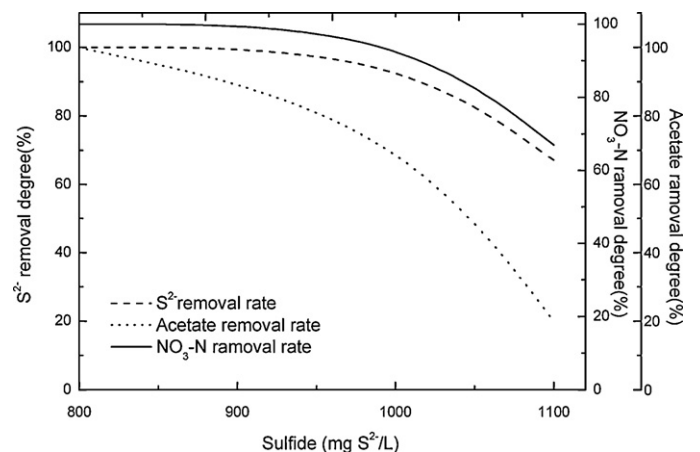


Fig. 5. Model simulation results for (a)  $S^{2-}$ , (b) acetate and (c)  $NO_3^-$ -N removal at  $S^{2-}$  concentrations of 800 mg/L, 1000 mg/L and 1100 mg/L.

0.84 kg-N/(m<sup>3</sup> d)). The removal of acetate–COD was decreased to 80% (1.90 kg-COD/(m<sup>3</sup> d)) at  $S^{2-} = 1000$  mg/L. However, the corresponding nitrate-N and sulfide-S removal were still complete (about 2.4 kg-S/(m<sup>3</sup> d), 1.05 kg-N/(m<sup>3</sup> d)). At  $S^{2-} = 1100$  mg/L, the acetate–COD removal rate was almost completely inhibited, only 20% was removed (about 0.53 kg-COD/(m<sup>3</sup> d)); while the nitrate-N and sulfide removal decreased to about 67% (about 1.76 kg-S/(m<sup>3</sup> d), 0.77 kg-N/(m<sup>3</sup> d)). Restated, the 1100 mg/L sulfide effectively inhibits the activity of heterotrophic denitrifier, leading

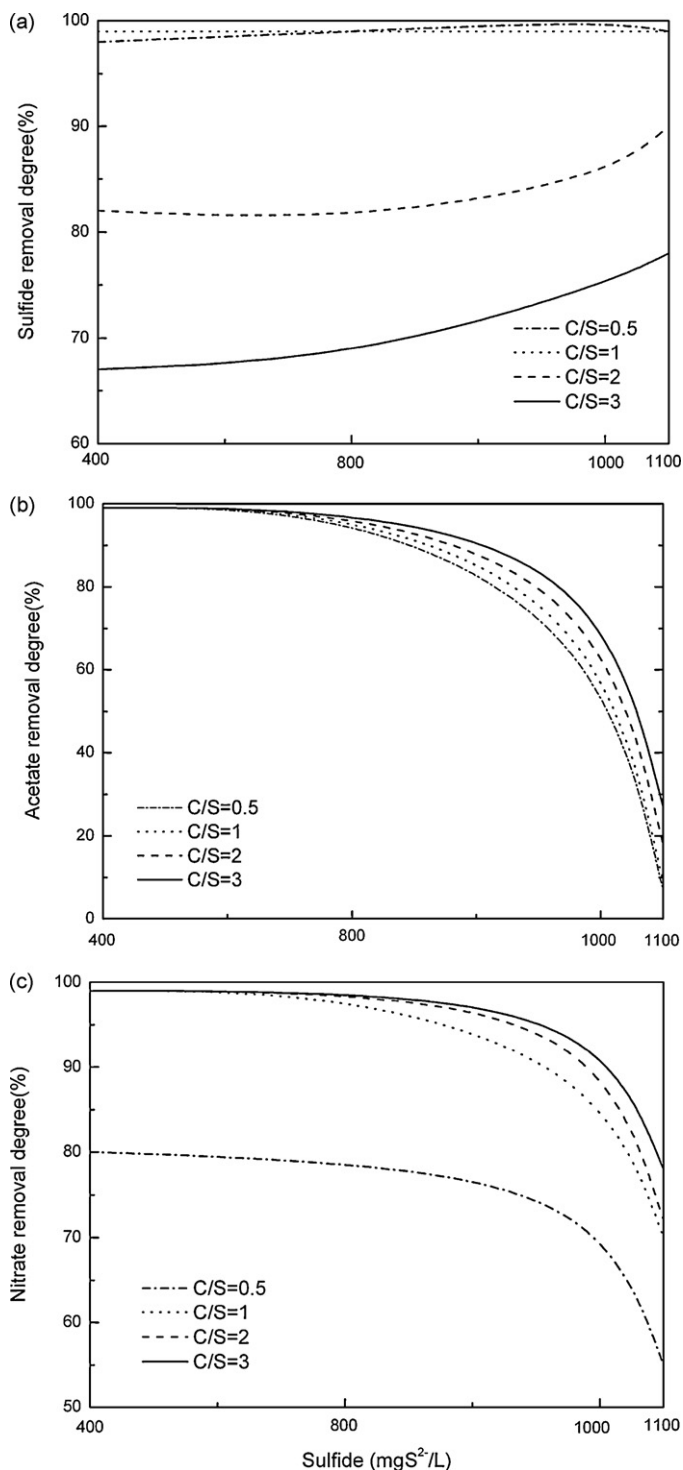


Fig. 6. Model simulation results for (a)  $S^{2-}$ , (b) acetate and (c)  $NO_3^-$ -N removal at C/S ratios of 0.5, 1, 2 and 3.

to an inhibition function of 0.4. The autotrophic denitrifier apparently tolerates high levels of influent sulfide concentration.

The impact of C/S on DSR performance at different sulfide concentrations is shown in Fig. 6. The removal rates of acetate and nitrate are increased with increasing C/S ratio and with decreasing influent sulfide concentration. At  $S^{2-} = 1000$  mg/L, the acetate removal rate was increased from 53% (0.64 kg-COD/(m<sup>3</sup> d)) at C/S=0.5–78% (5.61 kg-COD/(m<sup>3</sup> d)) at C/S=3.0. The corresponding nitrate removal rate is increased from 75% (0.39 kg-N/(m<sup>3</sup> d)) at C/S=0.5–96% (0.50 kg-N/(m<sup>3</sup> d)) at C/S=3.0. On the other hand, the sulfide removal rate is decreased with increasing C/S ratio and influent sulfide concentration. This may be due to that much more influent carbon made more electron acceptors ( $NO_3^-$ ) got by heterotrophic denitrifiers, then less for autotrophic. For instance, at  $S^{2-} = 400$  mg/L the sulfide removal rate was increased from 67% (0.64 kg-S/(m<sup>3</sup> d)) at C/S=3.0–98% (0.94 kg-S/(m<sup>3</sup> d)) at C/S=0.5. The model predicts a satisfactory DSR performance at  $0.5 < C/S < 3.0$  with influent sulfide concentration of 400–1000 mg/L. At  $> 1000$  mg/L influent sulfide, the DSR system will break down.

## 6. Conclusions

This paper developed for the first time the kinetic model for the DSR process on the basis of ASM1 Model. The DSR experiments were conducted in an EGSB at influent sulfide concentrations of 200–800 mg/L, and C/S ratio of 0.75–1.26 to calibrate the model parameters. The fit model correlates well with the DSR process dynamics. With the introduced inhibition function, the model reveals severe inhibition effects on the heterotrophic denitrifiers at  $> 1000$  mg/L, thus leading to reactor breakdown. This prediction correlates well with literature results. On the other hand, at  $0.5 < C/S < 3.0$  with influent sulfide concentration of 400–1000 mg/L, the DSR reactor can work satisfactorily.

## Acknowledgements

We gratefully acknowledge the supports by the National Nature Science Foundation of China (No. 50678049 and No. 50878062), and by the Key National Nature Science Foundation of China (No. 50638020).

## References

- [1] I. Manconi, A. Carucci, P. Lens, S. Rossetti, Simultaneous biological removal of sulphide and nitrate by autotrophic denitrification in an activated sludge system, *Water Sci. Technol.* 3 (2006) 91–99.
- [2] A. Wang, D. Du, N. Ren., J. van Groenestijn, An innovative process of simultaneous desulfurization and denitrification by *Thiobacillus denitrificans*, *J. Environ. Sci. Health A* 40 (2005) 1939–1949.
- [3] J. Reyes-Avila, J. Razo-Flores, Gomez, Simultaneous biological removal of nitrogen, carbon and sulfur by denitrification, *Water Res.* 38 (2004) 3313–3321.
- [4] C. Chen, N. Ren, A. Wang, Simultaneous biological removal of sulfur, nitrogen and carbon using EGSB reactor, *Appl. Microbiol. Biotechnol.* 78 (2008) 1057–1063.
- [5] H. Furumai, H. Tagui, K. Fujita, Effects of pH and alkalinity on sulfur-denitrification in a biological granular filter, *Water Sci. Technol.* 34 (1996) 355–362.
- [6] M. Henze, C.P.L.J. Grady, W. Gujer, G.V.R. Marais, T. Matsuo, A general model for single sludge wastewater treatment systems, *Water Res.* 21 (1987) 505–515.
- [7] M. Henze, C.P.L.J. Grady, W. Gujer, G.V.R. Marais, T. Matsuo, Activated Sludge Model No. 1, IAWPRC Scientific and Technical Report No. 1, IAWPRC, London, 1987.
- [8] D.J. Batstone, Anaerobic Digestion Model No. 1 (ADM1), International Water Association Scientific and Technical Report No. 13, IWA Publishing, 2002.
- [9] D.S. Lee, J.M. Park, Neural network modeling for on-line estimation of nutrient dynamics in a sequentially-operated batch reactor, *J. Biotechnol.* 75 (1999) 229–239.
- [10] M. Cote, B.P.A. Grandjean, P. Lessard, J. Yhibault, Dynamic modeling of the activated sludge process: improving prediction using neural networks, *Water Res.* 29 (1995) 995–1004.

- [11] S.E. Oh, Y.B. Yoo, J.C. Young, I.S. Kim, Effect of organics on sulfur-utilizing autotrophic denitrification under mixotrophic conditions, *J. Biotechnol.* 92 (2001) 1–8.
- [12] D.L. Lee, I.S. Lee, Y.D. Choi, J.H. Bae, Effects of external carbon source and empty bed contact time on simultaneous heterotrophic and sulfur-utilizing autotrophic denitrification, *Process Biochem.* 36 (2001) 1215–1224.
- [13] P. Reichert, *AQUASIM 2.0—User Manual. Computer Program for the Identification and Simulation of Aquatic Systems*, Swiss Federal Institute for Environmental Science and Technology (EAWAG), 1998.
- [14] W. Gujer, T.A. Larsen, The implementation of biokinetics and conservation principles in ASIM, *Water Sci. Technol.* 31 (1995) 257–266.
- [15] G. Insel, G. Celikyilmaz, E. Ucisik-Akkaya, K. Yesiladali, Z.P. Cakar, C. Tamerler, D. Orhon, Respiriometric evaluation and modeling of glucose utilization by *Escherichia coli* under aerobic and mesophilic cultivation conditions, *Biotechnol. Bioeng.* 96 (2007) 94–105.
- [16] B.C. Ricardo, R. Sierra-Alvarez, P. Rowlette, R.F. Elias, J. Gomez, J.A. Field, Sulfide oxidation under chemolithoautotrophic denitrifying conditions, *Biotechnol. Bioeng.* 95 (2006) 1148–1157.
- [17] I. Jubany, J.A. Baeza, J. Carrera, J. Lafuente, Respiriometric calibration and validation of a biological nitrite oxidation model including biomass growth and substrate inhibition, *Water Res.* 39 (2005) 4574–4584.